Weyl phases in point-group symmetric superconductors

Vasudha Shivamoggi[1] and Matthew J. Gilbert[2,3]

[1]*Department of Physics, University of Illinois, Urbana-Champaign, Urbana, Illinois 61801, USA*
[2]*Department of Electrical and Computer Engineering, University of Illinois, Urbana-Champaign, Urbana, Illinois 61801, USA*
[3]*Micro and Nanotechnology Laboratory, University of Illinois, Urbana-Champaign, Urbana, Illinois 61801, USA*

We study superconductivity in a Weyl semimetal with broken time-reversal symmetry and stabilized by a point-group symmetry. The resulting superconducting phase is characterized by topologically protected bulk nodes and surface states with Fermi arcs. The topological invariant governing the system is calculated using changes in eigenvalues of the point-group operator along high-symmetry momentum lines. We show that this invariant is determined by the Fermi surface topology of the Weyl semimetal. We discuss the effect of surface orientation and C_4-breaking strain as possible experimental consequences.

I. INTRODUCTION

The discovery of topological phases in noninteracting electron band structures has resulted in a wealth of interesting new systems.[1–5] For materials with fully gapped bands, it is possible to define a topological invariant that determines the number of protected surface states[6–8] and the quantized value of response functions such as the Hall conductivity in integer quantum Hall systems[1,9] or the magnetoelectric effect in strong topological insulators.[10,11] The invariant underlies the precise quantization of these response functions and the robustness of the surface states since its value does not change as long as the band gap does not close.

In addition to fully gapped insulators and superconductors, however, topological phases can occur in gapless systems when the bulk nodal structures are themselves protected.[12,13] This occurs in Weyl semimetals, where the bulk bands touch at separated pairs of points in the Brillouin zone known as Weyl nodes. In three dimensions (3D), these nodes are robust to gap-opening perturbations. They behave like monopoles of Berry curvature and can only be removed by pairwise annihilation when two nodes with oppositely charged monopoles merge.[14,15] The magnitude of the monopole is the topological invariant underlying a pair of Weyl nodes, and is determined by the Berry flux through a closed two-dimensional (2D) surface in momentum space that encloses a single node. Similar to the bulk invariant in gapped topological phases, the bulk Weyl nodes are manifested physically as surface states displaying Fermi arcs and an anomalous Hall effect.[16] Weyl nodes have been proposed to exist in the A phase[12] of ^{3}He and recently in several materials including pyrochlore iridates,[15,16] topological insulator-ferromagnet multilayers,[17,18] and HgCr$_2$Se$_4$.[19,20]

In superconductors, nodal topological phases have also been found in certain time-reversal-invariant (TRI) materials whose bulk gap closes at nodal lines or rings in momentum space.[21–23] CePt$_3$Si is one such noncentrosymmetric superconductor in which spin-orbit coupling is proposed to result in a mixed singlet-triplet pairing. The stability of line nodes in this material has been attributed to a nontrivial topological invariant of a one-dimensional (1D) loop in momentum space enclosing the nodal line. The system has surface states with unusual flat bands in a certain range of momentum determined by the bulk line nodes.

In this work, we extend the understanding of topological phases in nodal superconductors to systems with point nodes that break time-reversal symmetry (TRS).[24–27] Specifically, we study a superconducting model with double-Weyl nodes (with monopole strength of 2) and protected surface states displaying Fermi arcs. The model consists of a double-Weyl semimetal stabilized by C_{4h} point-group symmetry, and superconducting pairing terms that preserve the point-group symmetry. To argue that the nodes and surface states are protected, we derive a topological invariant for the superconductor. For a Weyl phase, the calculation has two steps: find each pair of bulk nodes, and sum the corresponding Berry monopoles. We derive a simple way to carry out each step using changes in the symmetry eigenvalues along high-symmetry momentum (HSM) lines in the Brillouin zone.

Interestingly, we find that the invariant for the superconducting Weyl nodes is determined by the Fermi surface topology of the normal state. Fermi surface topology studies have been previously used to characterize fully gapped, TRI superconductors.[28–31] For example, the $\mathbb{Z}_2$ invariant of a gapped, odd-parity TRI superconductor is determined by the number of TRI momenta enclosed by the Fermi surface.[28,30,31] We extend these Fermi surface studies to the time-reversal-breaking gapless structure of Weyl phases. The method is applied to a superconducting system whose pairing vanishes on HSM lines, as the C_4-invariant pairings do. In this case, finding bulk nodes in the superconductor becomes equivalent to finding the intersections of HSM lines with the Fermi surface of the parent material. Therefore, an invariant describing the existence and type of bulk nodes becomes a statement about the Fermi surface topology.

In Sec. II, we argue based on symmetry considerations that Weyl nodes are stable in 3D, time-reversal-breaking superconductors. We also prove that robust invariants can be constructed from symmetry eigenvalues even in the presence of bulk nodes. In Sec. III, we present a model for a C_{4h}-invariant double-Weyl semimetal. Pairing terms that respect this symmetry are calculated in Sec. IV, as well as surface states of the resulting Weyl superconductor. In Sec. V, we derive an expression for the topological invariant of the superconducting Weyl phase. The result is applied to another class of C_{4h}-invariant Hamiltonians and generalized to systems

with C_n in Sec. VI. Finally, we give experimental signatures in Sec. VII.

II. SUPERCONDUCTORS WITH POINT NODES

A. Stability of Weyl nodes in superconductors

We argue that Weyl nodes are stable in superconductors that break TRS by considering symmetry classes. Weyl nodes are pairs of bulk gap-closing points that are topologically protected. For a two-band model in a 3D system, the Hamiltonian near the Weyl nodes can be written as $H = v_x p_x \sigma^x + v_y p_y \sigma^y \pm v_z p_z \sigma^z$. The $\pm$ in front of the last term indicates that the two nodes have opposite chirality. Any further perturbation can only shift the location of the nodes but can not open a gap. The existence of Weyl nodes requires either time-reversal symmetry (TRS) or inversion to be broken, and in this work we consider systems without TRS.

Weyl nodes are topological defects in momentum space. Similar to vortices in real space, they may annihilate pairwise but are individually robust. It is desirable to find a topological invariant underlying a pair of Weyl nodes analogous to the vorticity of a vortex pair. Because of the presence of bulk nodes, a topological invariant can not be well defined over the full 3D Brillouin zone. Instead, it is useful to consider a lower-dimensional subset of the Brillouin zone that surrounds the nodal region. Since the subset is chosen by design to avoid the nodes, the system constrained to the subset is fully gapped. A topological invariant is defined on this lower-dimensional subset so that a nontrivial value of the invariant indicates enclosed nodes. The robustness of this invariant ensures that the nodes can not be eliminated except across quantum phase transitions. Gapless phases are therefore protected by topological invariants of lower-dimensional subsets that enclose the nodal region.

Topological phases have been classified into a periodic table that predicts the invariants allowed for a given spatial dimension and symmetry class.[4,5] We use this classification to first review the topological nature of TRI superconductors with nodal lines, then analyze superconductors with point nodes. In TRI superconductors, the Hamiltonian on generic subsets of the Brillouin zone breaks both TRS and particle-hole symmetry (PHS). However, the Hamiltonian satisfies a chiral symmetry defined as the product of TRS and PHS, and thus belongs to symmetry class AIII which has a nontrivial integer-valued invariant[4] in 1D. Nodal lines can be surrounded by a 1D loop in momentum space and are protected by the 1D invariant [Fig. 1(a)]. Furthermore, the surface states of the superconductor correspond to the nontrivial edge states on the 1D momentum subset, which are zero-energy states. These flat surface bands may seem surprising in a 3D system, but should be thought of as the edge modes of the 1D topological phase that is protected by the nodal line.[21–23]

Next, we turn to superconductors with Weyl nodes and show the stability of those that break time reversal. Weyl nodes are point nodes that are enclosed by a 2D subset of the Brillouin zone [Fig. 1(b)]. Class AIII has no nontrivial 2D topological invariant, so point nodes are unstable in TRI superconductors. For this reason, breaking inversion while preserving TRS is
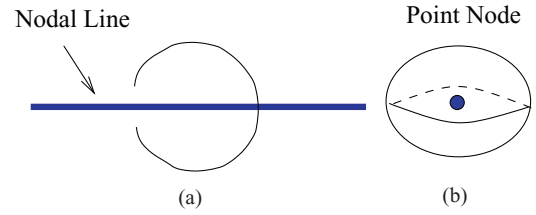

FIG. 1. (Color online) (a) A nodal line (blue) may be enclosed by a 1D loop (black) in momentum space. Topologically nontrivial nodal lines are protected by a 1D topological invariant defined on the enclosing loop, and are accompanied by the zero-energy states of the nontrivial 1D system. (b) A point node (blue) can be enclosed by a 2D surface (black), and is therefore protected by a nontrivial 2D invariant. The associated surface states are the linearly dispersing mid-gap states corresponding to a topologically nontrivial 2D system.

insufficient for a Weyl superconductor, although of course it is possible that additional symmetries may stabilize it.

For superconductors that break TRS, the Hamiltonian on generic subsets of the Brillouin zone again breaks TRS and PHS. In this case, there is no additional chiral symmetry, so the Hamiltonian on the subsets belongs to class A. The existence of a 2D topological invariant in class A makes Weyl nodes in TRS-breaking superconductors stable. The surface states correspond to the edge states of nontrivial 2D systems in class A, which are chiral and have linear dispersion. We verify this for the model studied in Sec. IV. Weyl nodes in superconductors breaking TRS therefore do not need additional symmetries to be stabilized. Our argument is in agreement with a previous microscopic calculation[25] showing that superconducting Weyl nodes are unstable in TRS systems but stable when TRS is broken. In this work, we use certain point-group symmetries to express the corresponding topological invariant in a simple way, although they are not necessary for the existence of the nodes.

B. Role of Fermi surface topology

We now show that symmetry eigenvalues can define a topological invariant even in the presence of generic bulk gap closings. Consider a two-band model

$$h_0 = d_1 \sigma^x + d_2 \sigma^y + d_3 \sigma^z, \tag{1}$$

where d_m are functions of momentum $\mathbf{k}$, and σ^m are Pauli matrices in a basis of spin, orbital, or spin-orbit-coupled degrees of freedom. A point-group operator η for a C_n, or n-fold, rotation about the z axis maps $\mathbf{k}$ to $U\mathbf{k} = (k_x \cos \frac{2\pi}{n} - k_y \sin \frac{2\pi}{n}, k_x \sin \frac{2\pi}{n} + k_y \cos \frac{2\pi}{n}, k_z)$. In this work, we consider a C_{4h} symmetry consisting of a combined fourfold rotation about the z axis and mirror reflection about the xy plane, which take (k_x, k_y, k_z) to $(k_y, -k_x, -k_z)$. A system that preserves this symmetry obeys

$$\eta h_0(\mathbf{k}) \eta^\dagger = h_0(U\mathbf{k}). \tag{2}$$

Without loss of generality, consider the case where the point-group operator is represented by σ^z. This leads to the following constraints on the coefficients of the Pauli matrices:

$$d_1(U\mathbf{k}) = -d_1(\mathbf{k}), \quad d_2(U\mathbf{k}) = -d_2(\mathbf{k}), \tag{3a}$$

$$d_3(U\mathbf{k}) = d_3(\mathbf{k}). \tag{3b}$$

We define high-symmetry momentum (HSM) points Γ_a as points in momentum space left invariant under the symmetry operator: $U\Gamma_a = \Gamma_a$. Evaluating Eq. (3a) at HSM gives $d_{1,2}(\Gamma_a) = -d_{1,2}(\Gamma_a)$, which implies that d_1 and d_2 vanish there. At these special points, the Hamiltonian takes the form

$$h_0(\Gamma_a) = d_3(\Gamma_a)\sigma^z, \qquad (4)$$

with energy eigenvalues $E(\Gamma_a) = \pm|d_3(\Gamma_a)|$. The Hamiltonian at HSM commutes with the symmetry operator, so each energy band can be characterized by eigenvalues of the symmetry operator ν_i:

$$\nu(\Gamma_a) = -\operatorname{sgn} d_3(\Gamma_a). \qquad (5)$$

The eigenvalue $\nu(\Gamma_a)$ changes sign only when $d_3(\Gamma_a)$ goes to 0, i.e., when the energy gap closes at one of the HSM. The product of symmetry eigenvalues $\chi = \prod_a \nu(\Gamma_a)$ can be used to define phases as regions of constant χ separated by gap closings at Γ_a. Since the $\nu(\Gamma_a)$ are defined only at HSM Γ_a, they do not change when the gap closes at non-high-symmetry points. Therefore, χ is a robust invariant even in the presence of bulk-gap closings, as long as they occur away from Γ_a.

In addition to defining a robust invariant for nodal systems, the symmetry eigenvalues can be used to detect and classify the nodes themselves. Consider rotation-invariant momentum lines, for example, $\mathbf{k}_\perp = (k_x, k_y) = (0,0)$ or (π, π) for C_4-invariant systems. Along a fixed $\mathbf{k}_\perp$, unequal values of ν at $k_z = 0$ and π indicate that the gap has closed at some value of k_z in-between. Formally, this difference is expressed as

$$\chi|_{\mathbf{k}_\perp} = \prod_n \frac{\nu_n(k_\perp, k_\perp, 0)}{\nu_n(k_\perp, k_\perp, \pi)}. \qquad (6)$$

This quantity is an invariant within each phase, and a value different from unity indicates the presence of a node (Fig. 2). In Sec. V, we will show that the specific value of $\chi_{\mathbf{k}_\perp}$ determines the Berry monopole strength of the nodes, for example, 2 for double-Weyl nodes.

This argument also applies to a superconductor with protected bulk nodes. Here, we show that examining symmetry eigenvalues at fixed $\mathbf{k}_\perp$ is equivalent in certain superconductors to studying the Fermi surface topology. Consider a point-group
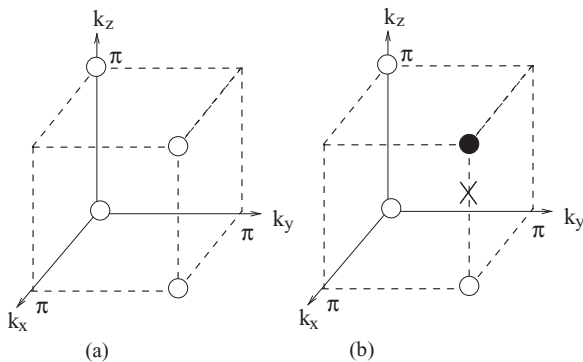

FIG. 2. Typical C_4 eigenvalue configurations for (a) an insulator and (b) a Weyl semimetal. The white (black) circles represent $\nu = +1$ (-1). The invariant $\chi_{\mathbf{k}_\perp}$ is the ratio of ν at $k_z = 0$ to ν at $k_z = \pi$ for fixed $\mathbf{k}_\perp$. A value of $\chi|_{\mathbf{k}_\perp} \neq 1$ indicates a bulk node (represented here by a cross) along the line $\mathbf{k}_\perp$. For the semimetal, $\chi_\pi = -1$, indicating a node along the $(k_x, k_y) = (\pi, \pi)$ line.

symmetric Weyl semimetal, and add pairing that respects the symmetry. The Hamiltonian of the superconductor is

$$H = H_0(\mathbf{k}) + \mu\tau^z + \Delta(\mathbf{k}), \qquad (7)$$

where $H_0(\mathbf{k})$ corresponds to the single-particle Hamiltonian h_0 from Eq. (1) after Bogoliubov–de Gennes (BdG) doubling, μ is the chemical potential, $\Delta(\mathbf{k})$ is the pairing matrix, and τ^i are the Pauli matrices in the electron and hole basis. As before, both $d_1(\Gamma_a)$ and $d_2(\Gamma_a)$ are required to vanish by the underlying point-group symmetry. Additionally, we consider pairing terms that vanish on rotationally invariant momentum lines. C_{4h}-invariant pairings satisfy this constraint, as will be shown in Sec. IV, however, the following argument applies to any pairing term that goes to zero along high-symmetry lines. This leaves two nonzero terms in the Hamiltonian at Γ_a: $d_3(\Gamma_a)$ and μ. The chemical potential commutes with the spin and orbital degrees of freedom represented by σ^m. At HSM, the energy bands are

$$E(\Gamma_a) = \pm[d_3(\Gamma_a) \pm \mu]. \qquad (8)$$

As a result of the simplified form of H at the HSM, we can again define an invariant in terms of symmetry eigenvalues

$$\nu'(\Gamma_a) = -\operatorname{sgn}[d_3(\Gamma_a) \pm \mu]. \qquad (9)$$

The eigenvalues change sign when the bulk gap closes at HSM, analogous to the semimetal. The key difference is that the gap closing occurs at $d_3(\Gamma_a) = 0$ in the semimetal and $d_3(\Gamma_a) = \pm\mu$ in the superconductor. For superconductors whose pairing vanishes on rotationally invariant momentum lines, the latter condition has a simple physical meaning in terms of the normal (nonsuperconducting) material. It marks the intersection of the parent Fermi surface with the rotationally invariant momentum lines. Therefore, bulk nodes in this type of superconductor are equivalent to intersections of HSM lines with the parent Fermi surface. Analogous to Eq. (6), an invariant $\chi|_{\mathbf{k}_\perp}$ is now written in terms of eigenvalues of the superconducting system [Eq. (7)]. As in the semimetal case, $\chi|_{\mathbf{k}_\perp}$ is different from unity in the presence of bulk nodes, and the exact value of $\chi|_{\mathbf{k}_\perp}$ determines the Berry monopole associated with the bulk nodes. The relation between $\chi|_{\mathbf{k}_\perp}$ and the bulk invariant describing Weyl nodes is the focus of Sec. V.

This argument does not depend on the specific form of the pairing term, other than that it vanishes at HSM. In this sense, the result is similar to previous work studying the effect of odd-parity pairing on topological insulators, where the topological invariant is determined by Fermi surface topology.[28–31] For example, the strong 3D index is equal to the number of enclosed TRI momenta modulo 2.[28,30,31] Weak indices are found using intersections of the Fermi surface with HSM, which for TRS are planes at $k_i = \pi$.[28,30] This is analogous to the invariants we construct using Fermi surface intersections with HSM lines to study Weyl nodes protected by a weak topological insulator phase.

III. DOUBLE-WEYL SEMIMETAL

We first discuss the properties of a double-Weyl semimetal with C_{4h} symmetry before considering pairing. We use the basis states $|\frac{3}{2}\frac{3}{2}\rangle$ and $|S, -\frac{1}{2}\rangle$ or, equivalently, $|c_{p_x+ip_y,\uparrow}\rangle$ and $|c_{s,\downarrow}\rangle$. These basis states are both eigenstates of angular

momentum with $J_z = \frac{3}{2}$ and $-\frac{1}{2}$, respectively. Physically, this is due to strong spin-orbit coupling, which couples lattice rotations to rotations in spin space. Under a C_4 rotation about the z axis, the orbitals transform as $p_x + ip_y \to -i(p_x + ip_y)$ and $s \to s$. Additionally, the spin $\uparrow$ and $\downarrow$ pick up factors of $e^{\mp i\pi/4}$, respectively. Putting both phases together, the C_{4h} operator in this basis has the form $e^{-\frac{3\pi i}{4}\sigma^z} U(\pi/2)$, where U maps (k_x, k_y, k_z) to $(k_y, -k_x, -k_z)$. There are four HSM defined by $k_x = k_y = 0$ or π and $k_z = 0$ or π.

Using this basis, we consider a two-band Hamiltonian following a derivation for $HgCr_2Se_4$ (Ref. [19]):

$$h_0 = (\cos k_x - \cos k_y)\sigma^x + \sin k_x \sin k_y \sigma^y$$
$$+ (m - \cos k_x - \cos k_y - \cos k_z)\sigma^z. \quad (10)$$

This model preserves a combined C_4 and M_z symmetry but breaks time-reversal symmetry, making it a 3D class A system. As expected when the symmetry operator is proportional to σ^z, the coefficients in front of σ^x and σ^y vanish at HSM. Equation (10) has bulk gap closings in a certain range of m: when $1 < m < 3$, the nodes are at $(k_x, k_y, k_z) = (0, 0, \pm k_0)$, where $k_0 = \cos^{-1}(m - 2)$. Similarly for $-3 < m < -1$, the nodes are at $(\pi, \pi, \pi \pm k_\pi)$ for $k_\pi = \cos^{-1}(m + 2)$. $1 < |m| < 3$ therefore corresponds to a phase with two distinct nodes that merge at the phase boundaries.

To see that this is a Weyl phase, we expand the Hamiltonian near the two nodes using $\vec{k} = (\delta k_x, \delta k_y, k_0 + \delta k_z)$ for $m > 0$ (the $m < 0$ case proceeds similarly):

$$h_0 \approx -\frac{1}{2}\delta k_-^2 \sigma^+ - \frac{1}{2}\delta k_+^2 \sigma^- \pm \sqrt{1 - (m-2)^2}\,\delta k_z \sigma^z, \quad (11)$$

where $k_\pm \equiv k_x \pm i k_y$ and $\sigma^\pm \equiv \sigma^x \pm i\sigma^y$. The $\pm$ in front of the last term in Eq. (11) indicates that the two nodes have opposite chirality. The Hamiltonian near the gapless points is quadratic in k_x and k_y. These two facts indicate that for $1 < |m| < 3$, the model has double-Weyl nodes.

A robust invariant for the Weyl semimetal can not be defined over the full 3D Brillouin zone because of the presence of nodes at two values of k_z. However, fixing k_z at a value away from the Weyl nodes results in a fully gapped 2D system for which a well-defined invariant does exist. As k_z is swept through various values, a change in the 2D invariant indicates a Weyl node. The magnitude of the change is equal to the strength of the associated Berry monopole. In the Weyl phase (e.g., $-3 < m < -1$), the 2D invariant is $C = 2$ in-between the Weyl nodes $\pi - k_\pi < k_z < \pi + k_\pi$, and $C = 0$ otherwise. The change in Chern number $|\Delta C| = 2$ is the topological invariant protecting the double-Weyl phase.

Apart from a few exceptions,[32,33] a nonzero value of a topological invariant is accompanied by robust surface states. We now show that 2D slices at fixed k_z where $C = 2$ have two chiral mid-gap states per surface, while those in the $C = 0$ range of k_z have no surface states. This momentum-dependent manifestation of the bulk-boundary correspondence results in the unusual Fermi arcs on Weyl surfaces. We consider surfaces parallel to the xz plane and calculate the spectrum of states localized in the y direction as a function of k_x for various values of fixed k_z. A previously derived method[34] expresses the existence of surface states as well as their dispersion in terms of parameters of the bulk Hamiltonian h_0 [Eq. (10)]. Using this method, it can be shown that the surface states exist
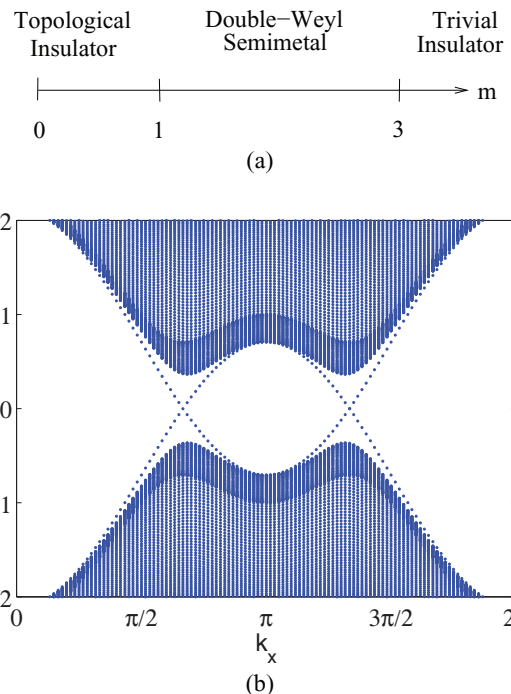

FIG. 3. (Color online) (a) Phase diagram of the model Hamiltonian (10) for $m \geqslant 0$ (the phases are symmetric about $m = 0$). For the insulating phases, the Chern number is well defined over the full Brillouin zone and takes the values $C = 2$ and 0 for the topological and trivial phases, respectively. For the double-Weyl semimetal phase, the invariant is the difference in Chern number on 2D momentum space slices separated by a Weyl node $\Delta C = 2$. (b) Energy bands of the double-Weyl semimetal with open boundaries in the y direction at fixed $k_z = \pi$ and $m = -2$. For this value of k_z, there are two chiral states per surface, indicating a topological invariant equal to 2.

in the following range of k_z:

$$\left|\tfrac{1}{2}(m - \cos k_z)\right| < 1. \quad (12)$$

This indicates that surface states exist when $|m| < 3$. Note that the range of mass m resulting in a Weyl semimetal $1 < |m| < 3$ is only a subset of the parameter space allowing surface states. The model therefore has more than one type of topological phase. The other phase, at $|m| < 1$, is a weak topological insulating phase [Fig. 3(a)].

For a value of k_z satisfying Eq. (12), the energy of the surface states can be found analytically[34] to be

$$E(k_x) = \pm\left[\cos k_x - \tfrac{1}{2}(m - \cos k_z)\right]. \quad (13)$$

Figure 3(b) shows both bulk and surface bands of the Weyl semimetal at $k_z = \pi$. There are two chiral states per surface, with degeneracies at $k_x = \pi \pm \cos^{-1}[(m + 1)/2]$. As k_z changes, the surface state degeneracies shift according to Eq. (13) until finally they merge at the Weyl nodes, $k_z = \pi \pm k_\pi$. As k_z is increased further into the region where $C = 0$, there are no surface states at all. Figure 4 shows a plot of the Fermi surface at $E = 0$ for $m = -2$. The dashed lines are two Fermi arcs terminating at the double-Weyl nodes. The bulk-boundary correspondence can therefore be formulated in Weyl phases as an equivalence between the number of robust
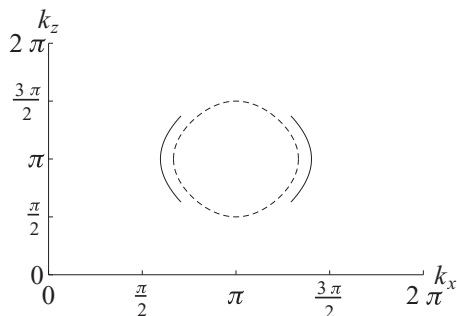
FIG. 4. Fermi arcs for $m = -2$. The dashed line corresponds to a C_4-invariant system, which has two Fermi arcs beginning and ending at the two double-Weyl nodes. The two nodes split into four double-Weyl nodes when a C_4-breaking term is added, and the Fermi arcs (solid lines) terminate at these four nodes. In this case, it is clear that the Fermi surface is comprised of open arcs.

Fermi arcs and the Berry monopole strength of the bulk Weyl node. The Fermi arcs arise because the surface states only exist for the range of k_z between the two Weyl nodes. The Weyl semimetal owes its existence to the topological insulator in this region. As m approaches ± 1 or ± 3, the two nodes approach one another and the range of k_z with $C = 2$ shrinks. It vanishes entirely at the phase boundaries when the Weyl nodes merge, and further changes in m result in a fully gapped phase.

The double-Weyl nodes can be thought of as two single-Weyl nodes with $\Delta C = 1$ that have merged and are kept together by C_4 symmetry.[20] If C_4 is broken, for example by adding the term $a_0\sigma^x$ to Eq. (10), each double-Weyl node splits into two single-Weyl nodes. Note that the Chern number C is still 2 for k_z between the Weyl nodes, indicating that the topological properties of the surface states are robust to C_4-breaking terms. The surface spectra shift so that the Fermi arcs terminate at the four single-Weyl nodes, seen as the solid lines in Fig. 4. Now it is clear that they are two disconnected arcs. The role of the point-group symmetry is to stablize multi-Weyl nodes in this model, but the topological phase itself does not depend on this symmetry for its existence. As we showed in Sec. II A, a 3D Hamiltonian in class A can support Weyl nodes without the need for additional symmetries. The motivation for considering point-group-symmetric models in this work is that the symmetry makes evaluating the invariant easier.

IV. C_4-INVARIANT PAIRING

We turn to a superconductor with Eq. (10) as its kinetic term and pairing that preserves C_{4h}. To be particle-hole symmetric, the Hamiltonian H must satisfy

$$\Xi H(k)\Xi^{\dagger} = -H^T(-k), \tag{14}$$

where Ξ is the PHS operator. For a general Hamiltonian of the form

$$H = \begin{pmatrix} h_e(\mathbf{k}) & \delta(\mathbf{k}) \\ \delta^{\dagger}(\mathbf{k}) & h_h(\mathbf{k}) \end{pmatrix}$$

and $\Xi = \tau^x$, PHS requires

$$h_h(\mathbf{k}) = -h_e^T(-\mathbf{k}), \tag{15a}$$

$$\delta(\mathbf{k}) = -\delta^T(-\mathbf{k}). \tag{15b}$$

The kinetic part of the Hamitonian becomes

$$H_0 = (\cos k_x - \cos k_y)\sigma^x\tau^z + \sin k_x \sin k_y\sigma^y$$
$$+ (m - \cos k_x - \cos k_y - \cos k_z)\sigma^z\tau^z + \mu\tau^z. \tag{16}$$

C_{4h} symmetry is expressed as

$$\eta H(k_x, k_y, -k_z)\eta^{\dagger} = H(k_y, -k_x, -k_z). \tag{17}$$

In the full electron-hole basis, the C_{4h} operator has the form

$$\eta = \begin{pmatrix} e^{-\frac{3\pi i}{4}} & & & \\ & e^{\frac{\pi i}{4}} & & \\ & & e^{\frac{3\pi i}{4}} & \\ & & & e^{-\frac{\pi i}{4}} \end{pmatrix}$$
$$= \frac{-1}{\sqrt{2}} U\left(\frac{\pi}{2}\right)(\sigma^z + i\sigma^z\tau^z). \tag{18}$$

We find four pairing terms that satisfy both PHS and C_{4h} [Eqs. (15b) and (17)]:

$$\Delta_1 = \Delta_0(\sin k_x\tau^x - \sin k_y\tau^y), \tag{19a}$$

$$\Delta_2 = \Delta_0(\sin k_x\sigma^x\tau^x - \sin k_y\sigma^x\tau^y), \tag{19b}$$

$$\Delta_3 = \Delta_0 \sin k_z(\sin k_x\sigma^y\tau^x - \sin k_y\sigma^y\tau^y), \tag{19c}$$

$$\Delta_4 = \Delta_0(\sin k_x\sigma^z\tau^x - \sin k_y\sigma^z\tau^y). \tag{19d}$$

The full Hamiltonian is $H = H_0 + \Delta_i$. The Hamiltonian for the C_{4h}-invariant superconductor is a four-band model with nodes shifted from the single-particle Weyl nodes to $[0, 0, \pm \cos^{-1}(m - 2 \pm \mu)]$ or $[\pi, \pi, \pi \pm \cos^{-1}(m + 2 \pm \mu)]$. Since all of the C_{4h}-invariaint pairings vanish along C_4-invariant momentum lines, they can not open a gap at the superconducting nodes.

As a first check on the protected nature of the superconducting nodes, we show that they are robust to gap opening in the same way as the single-particle nodes. The protection of the latter arises from the observation that a node of a two-band model written in terms of three Pauli matrices requires tuning three independent parameters. In 3D, the momenta provide a means to use up all possible mass terms, allowing for robust nodes. A four-band model can be written in terms of five mutually anticommuting 4×4 matrices, suggesting that Weyl behavior is possible in $D = 5$. However the nodes in our $D = 3$ model are protected as a result of the form of the kinetic part of the Hamiltonian (16). It can be shown that no matrix anticommutes with all three terms of H_0. Any term added to H_0 commutes with at least one term, which at most shifts the Weyl node.

The superconducting Weyl nodes are associated with surface states, and we present the spectrum with pairing Δ_2 [Eq. (19b)] as a representative example. Figure 5(a) shows the energy eigenvalues for $H = H_0 + \Delta_2$ with open boundaries in the y direction. The model parameters are the same as those in Fig. 3(b): $m = -2$ and $k_z = \pi$. Comparing with Fig. 3(b) shows that pairing splits each of the two surface states into two,
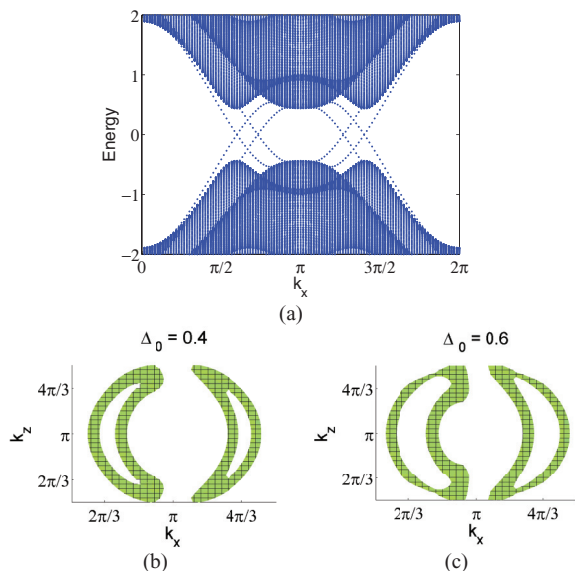
FIG. 5. (Color online) Surface spectrum and Fermi arcs with pairing term Δ_2 at $m = -2$. (a) Surface bands at fixed $k_z = \pi$ for $\Delta_0 = 0.4$. Comparison with Fig. 3(b) shows that pairing causes each single-particle surface state to split into two. The number of surface states, in this case 4, is protected by the bulk topological invariant of the superconducting system. (b) There are four Fermi arcs, in contrast to the two arcs in the absence of pairing (Fig. 4). The splitting of each pair of surface states increases with Δ_0. (c) Shows Fermi arcs at $\Delta_0 = 0.6$.

by an amount that grows with Δ_0. The spectra for Δ_3 and Δ_4 are similar, while Δ_1 results in two pairs of doubly degenerate surface states. The splitting (or lack thereof) can be understood as the response of the semimetal surface states to perturbations. Each pairing matrix commutes with at least one term in H_0 and shifts the energy eigenvalues accordingly. For the pairing in our example, $[\Delta_2, \sigma^z \tau^z] = 0$, and the corresponding bulk energies are written as

$$
E_2^2 = (\cos k_x - \cos k_y)^2 + (\sin k_x \sin k_y)^2
$$
$$
+ \left[m - \sum_i \cos k_i \pm \Delta_0 \sqrt{\sin^2 k_x + \sin^2 k_y} \pm \mu \right]^2 .
$$
(20)

Δ_2 enters the energy spectrum as two momentum-dependent perturbations of opposite sign $\pm \Delta_0 \sqrt{\sin^2 k_x + \sin^2 k_y}$ to the $\sigma^z \tau^z$ term in H_0. A constant perturbation $a_0 \sigma^z \tau^z$ shifts the surface states, in opposite directions for opposite signs of a_0. The effect of Δ_2 is to shift the surface states in opposite directions and cause a splitting proportional to Δ_0, as seen in Figs. 5(b) and 5(c). The same explanation applies to the effect of Δ_3 and Δ_4. However, Δ_1 enters the bulk energy spectrum as a perturbation to the σ^y term. It can be shown that adding a constant perturbation $a_0 \sigma^y$ leaves the surface states unshifted, and this qualitatively explains the twofold degeneracy of the surface states with Δ_1.

V. CALCULATION OF THE SUPERCONDUCTING INVARIANT

The superconducting Weyl nodes and surface states studied in the previous section are protected by a bulk topological invariant. We now calculate this invariant using changes in symmetry eigenvalues along HSM lines. We first derive a formula for the invariant for a semimetal in Sec. V A and then extend the analysis to a superconductor in Sec. V B.

A. Semimetal invariant

For a 3D system with C_4 symmetry in the xy plane, the Chern number C at a fixed value of k_z is given up to a gauge by

$$
e^{\frac{i\pi}{2} C} = \prod_{n \in occ} \xi_n(0, 0, k_z) \xi_n(\pi, \pi, k_z) \zeta_n(0, \pi, k_z), \quad (21)
$$

where ξ and ζ are C_4 and C_2 eigenvalues, respectively.[20] Equation (21) provides a simple way of computing the 2D invariant for any fixed value of k_z away from a node. Unequal values of C for two different k_z indicate Weyl nodes. According to the argument presented in Sec. II B, the nodes can be detected directly via changes in symmetry eigenvalues along HSM lines, i.e., at fixed $\mathbf{k}_\perp = (k_x, k_y)$ rather than k_z, as in Eq. (21). We now prove that these changes determine the type of Weyl node as well. The advantage of this alternative formula is that it brings to light the role of the parent material's Fermi surface topology in the superconducting case. From Eq. (21), the change in Chern number ΔC between $k_z = 0$ and π is

$$
e^{\frac{i\pi}{2} \Delta C} = \prod_{n \in occ} \frac{\xi_n(0,0,0)\xi_n(\pi,\pi,0)\zeta_n(0,\pi,0)}{\xi_n(0,0,\pi)\xi_n(\pi,\pi,\pi)\zeta_n(0,\pi,\pi)}. \quad (22)
$$

The eigenvalues of the C_4 and C_2 operators take the form $e^{i\pi s/2}$ and $e^{i\pi r}$, respectively, where s and r are integers. Two values of $\xi(\zeta)$ can be compared using their ratio $e^{i\pi(s_a - s_2)/2} \equiv e^{i\theta}(e^{i\phi})$. For convenience, we define $\theta_{k_\perp}$ as the phase difference of two eigenvalues ξ at the same $k_x = k_y = k_\perp$. Substituting these forms into Eq. (22) gives

$$
e^{\frac{i\pi}{2} \Delta C} = e^{i\theta_0} e^{i\theta_\pi} e^{i\phi}.
$$

The expression for ΔC is

$$
\Delta C = \frac{1}{\pi/2} \left(\phi + \sum_{k_\perp} \theta_{k_\perp} \right). \quad (23)
$$

The invariant for a C_4-invariant Weyl semimetal is thus determined by the relative phase of the symmetry eigenvalues across the node. Equation (23) computes the invariant in two steps. (1) Nodes are detected via changes in ξ or ζ. Along lines of fixed k_x and k_y, the eigenvalues ξ and ζ can only change when the bulk gap closes at some intermediate k_z. Therefore, a nonzero value of any of the phase changes $\theta_{k_\perp}$ or ϕ indicate a bulk node. (2) The Berry monopole strength is the sum of phase changes in ξ and ζ. Equation (23) shows how C_4 symmetry permits both single- and double-Weyl nodes. In models where ξ changes between $+1$ and -1, $\theta_{k_\perp} = \pi$ and $\Delta C = 2$ (double Weyl). On the other hand, single-Weyl nodes may occur when ξ changes between $+1$ and i, resulting in $\theta_{k_\perp} = \pi/2$ and $\Delta C = 1$.

We apply this result to the double-Weyl model studied in Sec. III. For the Hamiltonian h_0 in Eq. (10), the C_4 operator was found to be proportional to σ^z. $C_2 = C_4^2$ is then proportional to the identity, so the two bands have the same inversion eigenvalue. In this section, $\zeta(0,\pi,k_z)$ can therefore be set to 1 and dropped from the expressions. Define high-symmetry momenta (HSM) of the C_{4h} operation as $\Gamma_a = (k_\perp, k_\perp, k_{z_a})$, where $k_\perp$ and k_{z_a} can be 0 or π independently. Evaluating the Hamiltonian at HSM gives $h_0(\Gamma_0) = (m - 2\cos k_\perp - \cos k_{z_a})\sigma^z$, with C_4 eigenvalues $\xi(\Gamma_a) = -\mathrm{sgn}(m - 2\cos k_\perp - \cos k_{z_a})$. We use this expression to calculate the invariant in Eq. (23) at representative values of m.

At $m = 2$,

$$k_\perp = 0 : \xi(0,0,0) = 1, \quad \xi(0,0,\pi) = -1 \Rightarrow \theta_0 = \pi,$$
$$k_\perp = \pi : \xi(\pi,\pi,\pi) = -1, \quad \xi(\pi,\pi,\pi) = -1 \Rightarrow \theta_\pi = 0.$$

Substituting θ_0 and θ_π into Eq. (23) gives $\Delta C = 2$, indicating a double-Weyl semimetal at $m = 2$. The nonzero value of θ_0 additionally shows that the nodes occur along the $\mathbf{k}_\perp = (0,0)$ line. Repeating this for $m = 4$ gives

$$k_\perp = 0 : \xi(0,0,0) = -1, \quad \xi(0,0,\pi) = -1 \Rightarrow \theta_0 = 0,$$
$$k_\perp = \pi : \xi(\pi,\pi,\pi) = -1, \quad \xi(\pi,\pi,\pi) = -1 \Rightarrow \theta_\pi = 0.$$

Now $\Delta C = 0$, indicating an insulator at $m = 4$. We can determine the type of insulator by evaluating Eq. (21) at any value of k_z. All such 2D slices at $m = 4$ have $C = 0$, so this phase is a trivial insulator. Repeating this exercise at $m = 0$ shows an insulator with $C = 2$ at all values of k_z, corresponding to a topological insulator. The phase diagram in m [Fig. 3(a)] shows that the Weyl semimetal interpolates between trivial and topological insulator phases.

B. Superconducting invariant

The invariant for a C_{4h}-symmetric superconductor with Weyl nodes can be similarly written in terms of symmetry eigenvalues. To evaluate the invariant for Eq. (16) (independent of the choice of Δ_i), we must find an appropriate symmetry operator.[28,31] The operator $\tilde{\eta}$ is chosen to satisfy four constraints: (i) it is a symmetry operator of the Hamiltonian $\tilde{\eta}H(\mathbf{k})\tilde{\eta}^\dagger = H(U\mathbf{k})$; (ii) its eigenvalues $\tilde{\xi}$ are defined only at HSM of the C_{4h} symmetry; (iii) $\tilde{\xi}$ takes only the values of the single-particle C_{4h} operator; and (iv) when the gap closes, $\tilde{\xi}$ changes by the same phase as in the single-particle case. For example, $\tilde{\xi}$ must switch sign for the basis used in Eqs. (10) and (16). The C_{4h} operator in the BdG basis [Eq. (18)] satisfies constraints (i)–(iii) but not (iv). Of the other natural choices, σ^z and $\sigma^z\tau^z$, $\sigma^z\tau^z$ is the only one that meets all the requirements.

Once the appropriate symmetry operator is identified, calculating the invariant is simply a four-band version of the method derived in Sec. V A. The superconducting invariant is the sum of any phase changes in symmetry eigenvalues along HSM lines:

$$\Delta C_{\mathrm{SC}} = \frac{1}{\pi/2}\left(\phi_s + \sum_{k_\perp} \theta_{s,k_\perp}\right), \tag{24}$$

where ϕ_s and $\theta_{s,k_\perp}$ are defined for the superconducting system as ϕ and $\theta_{k_\perp}$ are for the semimetal. As before, a nonzero value of either ϕ_s or $\theta_{s,k_\perp}$ indicates a bulk gap closing. Additionally,

it is equivalent to intersections of HSM lines with the parent material Fermi surface in a superconductor with pairing that vanishes along those lines. Weyl phases in a C_{4h}-symmetric superconductor can therefore be characterized by the number of Fermi surface intersections of the parent material. Using $\tilde{\eta} = \sigma^z\tau^z$ gives $\Delta C_{\mathrm{SC}} = 4$, in agreement with the four chiral surface states seen in Fig. 5(a).

VI. ADDITIONAL CASES

Up to this point, we have studied a two-band model with C_4 eigenvalues of opposite sign. The other possibility[16] is for a relative phase of $\pi/2$, so that the C_4 and C_2 operators have the form

$$C_4 = \begin{pmatrix} 1 & \\ & i \end{pmatrix}, \quad P = C_4^2 = \begin{pmatrix} 1 & \\ & -1 \end{pmatrix}. \tag{25}$$

An example of a two-band model invariant under C_{4h} in this basis is

$$h_0 = \alpha \sin k_y \sigma^x + \alpha \sin k_x \sigma^y$$
$$+ (m - \cos k_x - \cos k_y - \cos k_z)\sigma^z. \tag{26}$$

h_0 has nodes at $[0,0,\pm\cos^{-1}(m-2)]$ for $1 < m < 3$ and $[\pi,\pi,\pi \pm \cos^{-1}(m+2)]$ for $-3 < m < -1$. Additionally, there are two sets of nodes at $(0,\pi,\pm\cos^{-1}m)$ and $(\pi,0,\pm\cos^{-1}m)$ for $|m| < 1$. Near the nodes for $1 < m < 3$, h_0 has the form

$$H \approx \alpha\delta k_y \sigma^x + \alpha\delta k_x \sigma^y \pm \sqrt{1-(m-2)^2}\delta k_z \sigma^z \tag{27}$$

indicating that these are single-Weyl nodes. The other nodes show similar behavior.

We can again use Eq. (21) to calculate invariants and derive a phase diagram for this model. In this case, the inversion eigenvalue must be included explicitly since it varies between the two bands. For $m = 2$, this procedure shows that $\xi(0,0,k_{z_a})$ changes from 1 to i, leading to $\theta_0 = \pi/2$ and $\Delta C = 1$. The latter indicates a single-Weyl pair. At $m = 0$, $\theta_0 = \theta_\pi = 0$ and $\phi = \pi$. These phase changes result in $\Delta C = 2$. By C_4 symmetry a single-Weyl pair at $\mathbf{k} = (\pi,0,\cos^{-1}m)$ must be accompanied by another pair at $\mathbf{k} = (0,\pi,\cos^{-1}m)$, leading to an invariant of 2. A phase diagram for this model is shown in Fig. 6.

It is possible to find four C_{4h}-invariant pairings in this basis and show that they vanish along $\mathbf{k}_\perp = (0,0)$ and (π,π). The invariant for the resulting Weyl superconductor can be
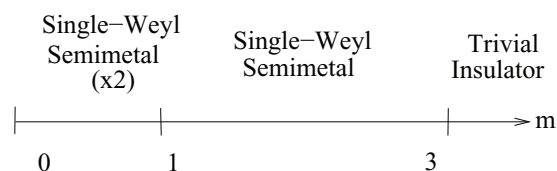

FIG. 6. Phase diagram of the model Hamiltonian (26) for $m \geqslant 0$ (the diagram is again symmetric about $m = 0$). Both nodal phases contain single-Weyl nodes. The $0 < m < 1$ phase has two single-Weyl pairs and therefore an invariant $\Delta C = 2$. For $1 < m < 3$, $\Delta C = 1$, consistent with one pair of single-Weyl nodes. The trivial nature of the insulating phase is confirmed by calculating the Chern number $C = 0$ according to Eq. (10).

found by choosing an appropriate symmetry operator and summing phase changes of its eigenvalues across Fermi surface intersections.

The simple form of the invariant [Eq. (23)] also makes it possible to generalize to systems with C_n symmetry. For the case of C_2, the Chern number is determined by the product of inversion eigenvalues.[32,33] In terms of phase changes ϕ, the invariant is

$$\Delta C = \frac{1}{\pi} \sum_{k_2} \phi_{k_2}, \qquad (28)$$

where k_2 is invariant under C_2 (e.g.,, $k_x = 0$ and $k_y = \pi$). Similarly, the Chern number of a C_3-symmetric system is given by the product of C_3 eigenvalues.[20] For α defined as the change in phase of a C_3 eigenvalue, the invariant is

$$\Delta C = \frac{1}{2\pi/3} \sum_{k_3} \alpha_{k_3}, \qquad (29)$$

where k_3 are the C_3-invariant momentum lines. Finally, the Chern number of a C_6-symmetric model is the product of a C_2, C_3, and C_6 eigenvalue.[20] It can be written as

$$\Delta C = \frac{1}{\pi/3} (\phi + \alpha + \beta), \qquad (30)$$

where β is the phase change of the C_6 eigenvalue.

VII. EXPERIMENTAL SIGNATURES

A. YPtBi

We propose strained YPtBi as a candidate for a C_4-invariant superconductor with topologically protected point nodes. YPtBi is a half-Heusler compound with a zinc-blende lattice. *Ab initio* studies[35] show that strong spin-orbit coupling in this material causes band inversion and results in a semimetal with a single quadratic band touching at the zone center Γ. This type of semimetal can be converted into a double-Weyl semimetal by applying strain that breaks cubic symmetry but preserves C_4 symmetry,[36] for example, uniaxial strain along the z axis.

YPtBi has a superconducting ground state, recently observed in experimental studies which found unconventional pairing and a semimetallic normal state.[37] The absence of inversion symmetry in this material can combine with the strong spin-orbit coupling to cause odd-parity pairing. A recent calculation has demonstrated that long-range attractive interactions in a Weyl semimetal can cause a superconducting state in which the odd-parity BCS term is the energetically favored pairing.[27] This provides a possible mechanism for the type of odd-parity BCS pairing term that we have analyzed in this work. For these reasons, we believe YPtBi with C_4-preserving strain is a good candidate for double-Weyl nodes in a superconducting system.

B. Surface states

Since the bulk density of states vanishes at the Weyl nodes, the surface states dominate the density of states near $E = 0$. Angle-resolved photoemission spectroscopy or scanning tunneling spectroscopy (STS) measurements are a direct way to probe the surface Fermi arcs. The superconductor with double-Weyl nodes has two pairs of arcs that split with Δ_0 as seen in Figs. 5(b) and 5(c), and this may provide a way to measure the strength of the pairing in the material.

An additional probe is the effect of strain that breaks C_4 symmetry. Under a strain that breaks C_4 symmetry, each double-Weyl node splits into two single-Weyl nodes (Fig. 4). In the superconducting case, the Fermi arcs split into four open pieces. The localized states also show a strong dependence on the orientation of the surface. The surface states shown in Figs. 3(b) and 5(a) are localized in the y direction. C_4 symmetry implies the same behavior for [100] surfaces. However, no robust surface states exist on [001] surfaces since there are no topologically nontrivial 2D slices that include the k_z axis.

VIII. CONCLUSION

We have studied topologically protected point nodes in superconductors that break time reversal and preserve C_4 symmetry. An argument based on symmetry classes shows that 3D time-reversal-breaking superconductors can support Weyl nodes with no additional symmetries, unlike TRI superconductors. We have used a model with C_{4h} symmetry that stabilizes double-Weyl nodes and allows the topological invariant of the system to be easily computed. The addition of pairing that obeys the same lattice symmetry results in a superconductor with two pairs of double-Weyl nodes. The topological invariant protecting this phase is calculated from changes in symmetry eigenvalues along HSM lines. Additionally, the expressions are generalized for systems satisfying C_n symmetry.

The advantage of comparing eigenvalues along HSM lines is that it provides insight into the role of the parent Fermi surface. We have shown that when the pairing terms vanish along C_4-invariant momentum lines, point nodes in the superconductor are equivalent to intersections of the HSM lines with the Fermi surface of the *parent material*. The role of Fermi surface topology in determining topological invariants has been studied in gapped TRI superconductors with odd pairing. We have shown that it is similarly pivotal in gapless phases where the invariant protects the nodal structure itself. This result highlights the importance of Fermi surface topology in the search for unconventional or odd-parity pairing.

[1] D. J. Thouless, M. Kohmoto, M. P. Nightingale, and M. den Nijs, Phys. Rev. Lett. **49**, 405 (1982).

[2] M. Z. Hasan and C. L. Kane, Rev. Mod. Phys. **82**, 3045 (2010).

[3] X.-L. Qi and S.-C. Zhang, Rev. Mod. Phys. **83**, 1057 (2011).

[4] A. P. Schnyder, S. Ryu, A. Furusaki, and A. W. W. Ludwig, Phys. Rev. B **78**, 195125 (2008).

[5] A. Kitaev, AIP Conf. Proc. **1134**, 22 (2009).

[6] R. B. Laughlin, Phys. Rev. B **23**, 5632 (1981).

[7] B. I. Halperin, Phys. Rev. B **25**, 2185 (1982).

[8] L. Fu and C. L. Kane, Phys. Rev. B **74**, 195312 (2006).

[9] J. E. Avron, R. Seiler, and B. Simon, Phys. Rev. Lett. **51**, 51 (1983).

[10] X.-L. Qi, T. L. Hughes, and S.-C. Zhang, Phys. Rev. B **78**, 195424 (2008).

[11] A. M. Essin, J. E. Moore, and D. Vanderbilt, Phys. Rev. Lett. **102**, 146805 (2009).

[12] G. E. Volovik, *The Universe in a Helium Droplet* (Clarendon, Oxford, 2003).

[13] A. M. Turner and A. Vishwanath, arXiv:1301.0330.

[14] S. Murakami, New J. Phys. **9**, 356 (2007).

[15] X. Wan, A. M. Turner, A. Vishwanath, and S. Y. Savrasov, Phys. Rev. B **83**, 205101 (2011).

[16] K.-Y. Yang, Y.-M. Lu, and Y. Ran, Phys. Rev. B **84**, 075129 (2011).

[17] A. A. Burkov and L. Balents, Phys. Rev. Lett. **107**, 127205 (2011).

[18] G. B. Halász and L. Balents, Phys. Rev. B **85**, 035103 (2012).

[19] G. Xu, H. Weng, Z. Wang, X. Dai, and Z. Fang, Phys. Rev. Lett. **107**, 186806 (2011).

[20] C. Fang, M. J. Gilbert, X. Dai, and B. A. Bernevig, Phys. Rev. Lett. **108**, 266802 (2012).

[21] M. Sato, Phys. Rev. B **73**, 214502 (2006).

[22] B. Béri, Phys. Rev. B **81**, 134515 (2010).

[23] A. P. Schnyder and S. Ryu, Phys. Rev. B **84**, 060504 (2011).

[24] J. D. Sau and S. Tewari, Phys. Rev. B **86**, 104509 (2012).

[25] T. Meng and L. Balents, Phys. Rev. B **86**, 054504 (2012).

[26] G. Y. Cho, J. H. Bardarson, Y.-M. Lu, and J. E. Moore, Phys. Rev. B **86**, 214514 (2012).

[27] H. Wei, S.-P. Chao, and V. Aji, arXiv:1305.7233.

[28] M. Sato, Phys. Rev. B **79**, 214526 (2009).

[29] X.-L. Qi, T. L. Hughes, and S.-C. Zhang, Phys. Rev. B **81**, 134508 (2010).

[30] M. Sato, Phys. Rev. B **81**, 220504 (2010).

[31] L. Fu and E. Berg, Phys. Rev. Lett. **105**, 097001 (2010).

[32] T. L. Hughes, E. Prodan, and B. A. Bernevig, Phys. Rev. B **83**, 245132 (2011).

[33] A. M. Turner, Y. Zhang, R. S. K. Mong, and A. Vishwanath, Phys. Rev. B **85**, 165120 (2012).

[34] R. S. K. Mong and V. Shivamoggi, Phys. Rev. B **83**, 125109 (2011).

[35] W. Al-Sawai, H. Lin, R. S. Markiewicz, L. A. Wray, Y. Xia, S.-Y. Xu, M. Z. Hasan, and A. Bansil, Phys. Rev. B **82**, 125208 (2010).

[36] E.-G. Moon, C. Xu, Y. B. Kim, and L. Balents, arXiv:1212.1168.

[37] N. P. Butch, P. Syers, K. Kirshenbaum, A. P. Hope, and J. Paglione, Phys. Rev. B **84**, 220504 (2011).